Design of All-Optical Logic Gates Using NAND Gate in Photonic Crystal Waveguides

A Dissertation submitted towards the Partial Fulfillment of Award of Degree of

MASTERS OF TECHNOLOGY

In

NANOSCIENCE AND TECHNOLOGY

Submitted by

SHIBA FATIMA

2K14/NST/15

Under the Supervision of

Dr. Yogita Kalra

Assistant Professor

Department of Applied Physics

DEPARTMENT OF APPLIED PHYSICS

DELHI TECHNOLOGICAL UNIVERSITY

Main Bawana Road, Shahabad Daulatapur, New Delhi – 110042

JUNE-2016

DEPARTMENT OF APPLIED PHYSICS

DELHI TECHNOLOGICAL UNIVERSITY, NEW DELHI -110042

CERTIFICATE

This is to certify that this dissertation titled "**Design of All-Optical Logic Gates Using NAND Gate in Photonic Crystal Waveguides"** is the authentic work carried out by **SHIBA FATIMA** bearing Roll No. 2K14/NST/15, a student of Delhi Technological University, in the partial fulfillment of the requirement for the award of Degree in **Master of Technology** in "**Nano Science and Technology"**. As per the declaration of the student this work has not been submitted to any university/institution for the award of any degree/diploma.

Dr. Yogita Kalra

Project Guide

Department of Applied Physics

Delhi Technological University, New Delhi.

Prof. Suresh C. Sharma

Head of Department

Department of Applied Physics

Delhi Technological University, New Delhi

ACKNOWLEDGEMENT

A dissertation cannot be completed without the help of many people who contribute directly or indirectly through their constructive criticism in the evolution and preparation of this work. It would not be fair on my part, if I don't say a word of thanks to all those whose sincere advice made this period a real educative, enlightening, pleasurable and memorable one.

First of all, a special debt of gratitude is owned to my supervisor, Dr. Yogita Kalra for her gracious efforts and keen pursuits, which has remained as a valuable asset for the successful completion of research work. Her dynamism and diligent enthusiasm has been highly instrumental in keeping my spirit high. The flawless and forthright suggestions blended with an innate intelligent application have crowned my task a success.

I also like to offer my sincere thanks to all faculty members, teaching and non -teaching staff of Department of Applied Physics (AP), and staff of central library, DTU, Delhi for their assistance.

I am extremely thankful to my parents and friends for their constant encouragement during the entire course of my research work.

SHIBA FATIMA (2K14/NST/15)

M.Tech, Nano Science and Technology

Department of Applied Physics

Delhi Technological University, Delhi.

TABLE OF CONTENT

ABSTRACT

In this thesis, we have proposed the design of all-optical logic gate using the combination of universal NAND gates. The structure consists of hexagonal arrangement of air holes in silicon having a refractive index of 3.5. The radius of air holes has been taken as 0.3a, where 'a' is the lattice constant. The NAND gate has two input ports, one reference port and one output port. Initially, a single NAND gate structure has been optimized with a hole of radius 0.2a at the junction of all the four waveguides of NAND gate. The bends in the NAND gate have been optimized such that there are minimum bend losses. For this purpose six air holes of radius 0.15a have been placed at outer edge of the waveguide and radius of the inner edge hole has been reduced to 0.17a. Further, the optimized NAND gates that are the universal gates have been arranged in a combination such that the combined structure behaves as an all-optical logic gate. The proposed structure exhibits a response period of 6.48ps and bit rate of 0.154 Tb/sec. Thus, we have designed the all-optical logic gate with the help of universal NAND optical logic gate.

LIST of FIGURES

LIST of TABLES

CHAPTER 1
INTRODUCTION

1.1 THESIS APPROACH :

This thesis proposes the design of two dimensional (2-D) photonic crystal structures which consist of triangular lattice of air holes in silicon. Optical NAND gate has been designed and basic gates i.e. optical AND, OR, NOT, XOR and XNOR logic gates have been designed using the universal optical NAND gate combination. The response time and the bit rate of the designed structure have also been calculated. Optical logic means use of light in logic gates (NOT, AND, OR, NAND, NOR, XOR, XNOR). The structure has been designed and analyzed using 'BandSolve' and 'Fullwave' module of commercially available 'R-Soft' software.

1.2 THESIS OBJECTIVE :

The main objectives of this thesis work are as follows:

- To study the basics of photonic crystal and its types.
- To study the light guidance in photonic crystal waveguide and the introducing defects i.e. line defect and point defect in photonic crystals.
- To study the properties of photonic bandgap and the factors affecting it.
- To explore the possibilities of designing photonic optical logic gates.
- To design and analyze the optical NAND logic gate and other basic gates from the combination of universal optical NAND logic gate.

1.3 THESIS ORGANIZATION :

This thesis work is summed up into five chapters. Chapter 1 gives the brief introduction of the thesis and its objectives. Chapter 2 includes the basics of photonic crystals and light guidance in photonic crystal structures. Literature review and the comparison of electronics and optics are covered in chapter 3. Chapter 4 includes the design, simulation and the results of the proposed optical NAND logic gate and the other optical logic gates designed using the combination of the

universal optical NAND logic gate. The conclusion and the future scope of this work are included in chapter 5.

CHAPTER 2
REVIEW OF LITERATURE

2.1 INTRODUCTION

Have you ever wondered what exactly happens to electrons in the semiconductor crystals or more so in particular, the photonic crystals? If not then consider these essentials. Forbidden energy states are there in a bandgap of the photonic crystal and because of the interference of electron wave functions in crystal lattice certain effects can be observed. Scattering at periodically arranged 'dielectric atoms' might leads to an optical band structure, which fundamentally changes the propagation of light, also the emission and absorption processes in these artificial structures. So it would be good to consider a close analogy of photons in so-called photonic crystals with other such related phenomena in the InGAS range of spectrum i.e. 1.3 to 1.8 μm [1].

The term 'Photonic Crystal' and the theory of the photonic bandgap [2, 3] were first introduced by Eli Yablonovitch in 1989; however, the idea of a 1-dimensional stop band was derived by Lord Rayleigh in the year 1887. These novel structures have become a topic of interest in the past few years with the aim of controlling the optical properties of materials. Enormous amount of research in this field has resulted in the technological advancements in many areas such as communications, optics, quantum information processing, and bio-sensing. Photonic crystals are periodic dielectric structures that have lattice spacing comparable to the wavelength of light [1, 2]. These periodic dielectric structures affect the dispersion relations and the spatial distribution of light travelling through the PhCs. There exist several analogies between the photonic crystals and the more familiar electronic crystals. The Brillouin zone which reflects the symmetry of real space crystals can illustrate the reciprocal lattice in both the electronic and photonic crystals. Also, photonic crystals can be defined as 'periodic dielectric structures that allow storage and wave-guiding of light through Bragg reflections'. Such structures can be used to engineer cavities whose mode volumes are on the order of light's wavelength. These cavities facilitate the interaction of light with matter resulting in quantum-optical phenomena such as spontaneous emission enhancement, strong coupling, and single atom lasers. Photonic crystals are usually viewed as an optical analogy to solid state crystals [4], in that the periodic arrangement of atoms in a crystal gives rise to the energy bandgaps. These energy bands control the motion of charge carriers through the crystal, which can

be altered by adding dopants. This has led to the creation of semiconductor devices such as transistors, diodes, and semiconductor lasers. Similarly, photonic crystal cavities also have bandgaps in which propagation of a certain frequency range of electromagnetic waves (light) is forbidden. Analogous to adding dopants in semiconductors, localized states within the photonic bandgaps are introduced by intentionally breaking the periodicity in adding defects or distortions to the crystal. Therefore, by engineering the properties of defects, one is capable of tuning and controlling the flow of light through the crystal [5].

2.2 TYPES OF PHOTONIC CRYSTAL

Photonic Crystals have been put through a large number of processes in recent years and are used in a broad range of industries from optics to communications. Photonic crystals can be primarily classified under three groups based on the periodicity of the dielectric material along one or more axes: One Dimensional Photonic Crystals (1-D PhCs), Two Dimensional Photonic Crystals (2-D PhCs) and Three Dimensional Photonic Crystals (3-D PhCs).

2.2.1 ONE DIMENSIONAL PHOTONIC CRYSTALS

The simplest possible PhC, as shown in Fig. 2.1 on the next page, consists of alternating layers of the material with different dielectric constant. The term "1-Dimensional" is used because the dielectric varies along one direction only. This type of multilayer film is termed as the one dimensional photonic crystal, which is very similar to a Bragg Stack . Lord Rayleigh (1887) published one of the first analyses of the optical properties of multilayer films. This type of PhCs can act as a mirror (a Bragg mirror) for light with a frequency within the specified range, and it can localize light modes if there are any defects in its structure. These concepts are commonly used in dielectric mirrors and optical filters (e.g. Hecht and Zajac, 1997). Now if a wave packet is incident normal to this 1-D structure, i.e. perpendicular to first flat face, the transmittance so obtained is as shown in Fig. 2.2 on the next page. Normalized frequency is used in the spectra shown in figure 2.2 and defined as the ratio of that particular frequency to the center frequency.

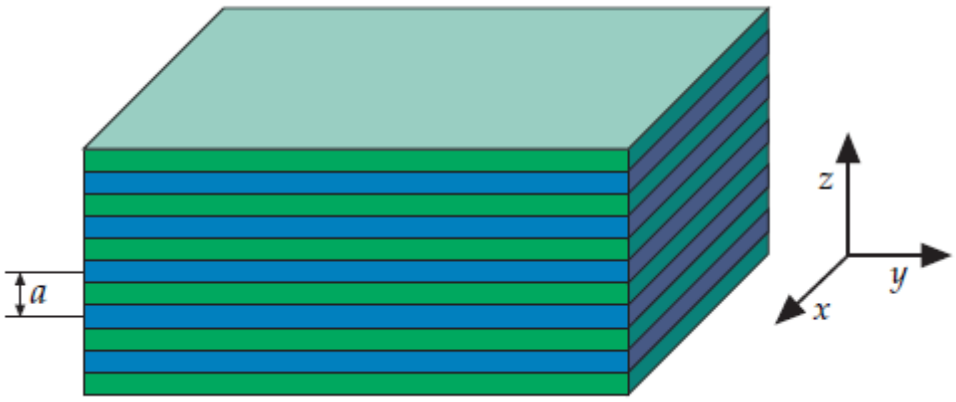

Figure 2.1 Structure of a One Dimensional Photonic Crystal

[Image source: J. D. Joannopoulos, S. G. Johnson, J. N. Winn, R. D. Meade, "Photonic Crystals - Molding the low of light", 2nd Edition, Princeton University Press, 2008.]

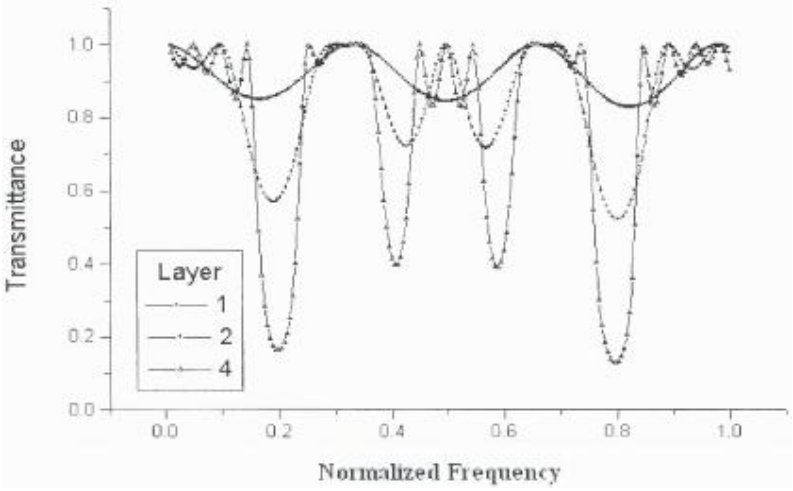

Figure 2.2 Transmittance Vs Normalized Frequency for a few layers of the crystal

[Image Source: "Optical properties of PhCs by A Shenoy"]

It can be seen in Figure 2.2, that with the increase in crystal thickness, the transmission response for some of the frequencies rapidly approaches zero. However, at the same time, widths of these troughs decrease. One-dimensional (1-D) photonic crystals are actually made to offer either reflection or anti-reflection coatings and this can be done by careful selection of the materials used, their thickness and number of layers. As the dielectric contrast increases, the photonic band gap exhibited by one dimensional photonic crystal also increases. It is evident from the figure 2.3 that

the width or the thickness of the layer when kept constant, photonic bandgap becomes larger as the dielectric contrast increases.

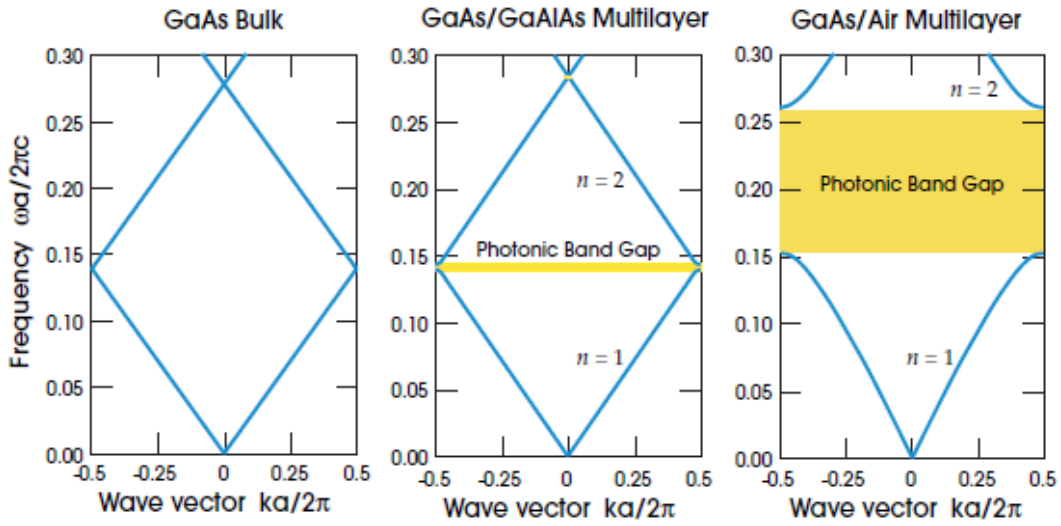

Figure 2.3: The photonic band structures for on-axis propagation, as computed for three different multilayer films. In all the three cases, each layer has a width of 0.5a. Left: every layer has same dielectric constant ε=13. Center: layers alternate between ε of 13 and 12. Right: layers alternate between ε of 13 and 1.

[Image source: J. D. Joannopoulos, S. G. Johnson, J. N. Winn, R. D. Meade, "Photonic Crystals - Molding the low of light", 2nd Edition, Princeton University Press, 2008.]

2.2.2 TWO DIMENSIONAL PHOTONIC CRYSTALS

There is a considerable interest in these two dimensional structures at present. There are numerous types of two dimensional lattice structures, namely - hexagonal lattice, square lattice, honeycomb lattice, etc.

A two-dimensional photonic crystal is periodic along only any two of its axes and homogeneous along the remaining axis. A typical example, consisting of dielectric columns is shown in figure 2.4. It is imagined that the columns are infinitely tall and the case of a finite extent in this direction falls in the category of the three dimensional photonic crystals. For some values of the columns spacing, the crystal will have a photonic band gap in xy plane.

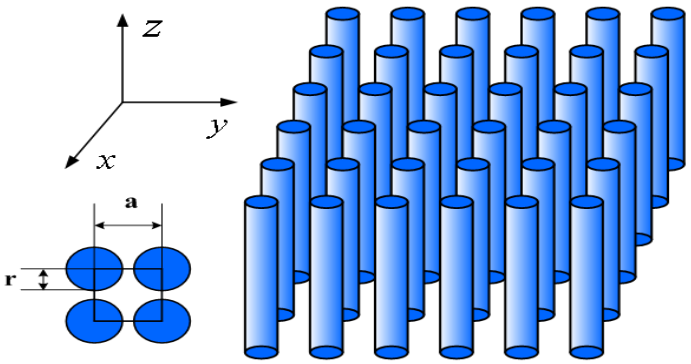

Figure 2.4 A two-dimensional photonic crystal. This material is a square lattice of dielectric column, with radius r and dielectric constant ε. The material is homogenous along the z direction (we imagine the cylinders are very tall), and periodic along the x and y with lattice constant a. The left inset shows the square lattice from above, with the unit cell framed in square shaped.

[Image source: J. D. Joannopoulos, S. G. Johnson, J. N. Winn, R. D. Meade, "Photonic Crystals - Molding the low of light", 2nd Edition, Princeton University Press, 2008.]

A two-dimensional (2-D) gap implies that if the wave is allowed to incident on the structure from any which direction within the same 2-D plane as the periodicity of the crystal, then it is observed that it will always be reflected. This, certainly, is limited to a specific range of frequencies. But still quite appreciable band-width [1] ('band width = gap width / central gap frequency') can be achieved. The repetitive rows of periodically arranged cylinders ensure that the two dimensional (2D) periodicity holds in only one of the plane. Therefore, if the incident radiation is supposed to restrict to this plane, then for correct filling ratios [1] and the material constants and the polarization of the wave, a complete two-dimensional (2-D) bandgap can be observed.

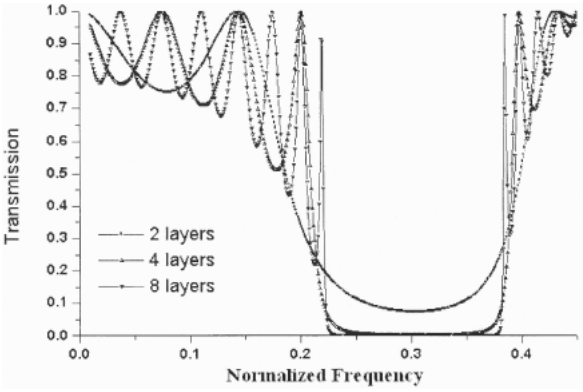

Figure 2.5 Transmission V/s Normalized Frequency for a two-dimensional Lattice Perfect Structure

[Source: "Optical properties of PhCs by A Shenoy"]

The graph for the transmission versus normalized frequency for a two dimensional perfect lattice is shown in Fig. 2.5. The region where there is normally zero transmission no spikes occur indicating a perfect lattice. If defect is introduced in the lattice spikes are witnessed the zero transmission region.

2.2.3 THREE DIMENSIONAL PHOTONIC CRYSTALS

Three-dimensional photonic crystals are the one which have periodicity in dielectric structure along the three different axes. They provide three-dimensional gaps. This states that any wave from any direction will be entirely reflected. The three dimensional PhCs may provide a novel reflector technology that can easily be scaled in a size so as to fit almost all intended applications. Take, for example, the first structure shown in figure 2.5. A periodic pattern is etched onto each of the wafers. These wafers are then stacked with alternating orthogonal orientations. This results in a woodpile like structure which has a complete band gap. In figure 2.6, an fcc lattice of dielectric spheres in which the unit cell has a sphere at each of the 8 vertices, as well as in the center of each of the cube faces, does not show up a complete band gap. The inverse opal structure i.e. fcc air holes in high dielectric can have a complete photonic band gap. Vlasov et al. (2001) were the first one to fabricate inverse opal structure in order to have a complete band gap.

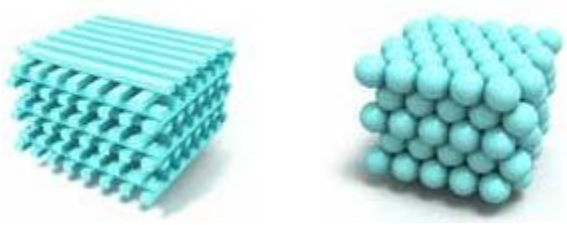

(a) (b)

Figure 2.6 Structure of the lattice for (a) woodpile and (b) opal

2.3 PHOTONIC BANDGAP

Although so-called one-dimensional photonic bandgap structures have been known commonly as Bragg mirrors for centuries, the proposition of the existence of a photonic bandgap (PBG) for multidimensional, periodic dielectric lattices by Yablonovitch and John in 1987 [6] paved the way

for a new category of optical materials which control the propagation of electromagnetic waves by creating bands of forbidden states in specified regions of dielectric. The photonic bandgap can be seen as an optical analogue to the electronic bandgaps present in crystalline semiconductors and insulators, where certain ranges of energies are not accessible to propagating electrons or holes. The electronic band diagrams, which plot the energy eigenvalues of the electron wavefunction, are found by solving Schrodinger's equation in a Bloch wave basis. Bloch waves are used due to the periodic potential of the atoms in the crystalline lattice, and the atomic size scale necessitates the application of quantum mechanics. Conversely, in a photonic bandgap material, the bands arise from the crystal-like periodicity of the dielectric material. Hence, materials that possess a photonic bandgap are often referred to as Photonic Crystals (PhC). The bandgap consists of a range of photon energies where light propagation is forbidden. Photons with energies falling within the bandgap decay exponentially into the PhC and are nearly totally reflected. The energy eigenvalues which are plotted in the photonic band structure correspond to the electromagnetic modes of the photonic crystal. Thus the existence of photonic band gap give rise to various interesting as well as useful properties like localization of light defects and surfaces and the inhibition of radiation. So, study of photonic band gap becomes necessary in order to take maximal advantage of the photonic crystals to control electromagnetic radiation. The bandgap in photonic crystals depends upon various parameters including the arrangement and size of the constituent air holes/dielectric rods, dielectric contrast of the two mediums that are being used in forming the photonic crystal and the fill factor.

2.4 FORMULATION OF THE MASTER EQUATION

In order to find the solutions to spatial part of the fields which are known as the mode profiles, Maxwell's equations are used. The size scale of the periodicity in PhCs, for example, a photonic bandgap in the near-infrared range requires periodicity of the dielectric function on the order of a few hundred nanometers while a photonic bandgap in the terahertz region requires millimeter-scale periodicity, is usually determined by the wavelength range of interest. Maxwell's equations include built-in scalability, which allows for the formation of photonic bandgaps in wavelengths ranging from the visible to microwave, and they are the basis for formulating the "master equation" [1] for solving modes of the crystal. To obtain the master equation it is assumed that:

(1) the mixed dielectric medium in question is void of free charges and currents, so ρ = 0 and J = 0;
(2) field strengths are small enough that high order terms in the electric susceptibility χ can be ignored; that is, no non-linear effects are considered;
(3) the material is macroscopic and isotropic;
(4) the frequency dependence of the dielectric constant (material dispersion) can be neglected; and
(5) the material is assumed to have purely real and positive ε(r) for all positions in space r.

With these assumptions in place, the time and spatially varying Maxwell equations are as follows:

$$\nabla . [\varepsilon(r)E(r,t)] = 0 \qquad \nabla \times E(r,t) + \mu_o \frac{\partial H(r,t)}{\partial t} = 0$$

$$\nabla . H(r,t) = 0 \qquad \nabla \times H(r,t) - \varepsilon_0 \varepsilon(r) \frac{\partial E(r,t)}{\partial t} = 0 \qquad (2.1)$$

where ε(r) represents the dielectric function in space. Note that ε_0 is divided out of the divergence terms due to the right side of the equation being 0. Next, the solutions are assumed to vary sinusoidally in time (harmonically), resulting in complex exponential solutions of the form:

$$H(r,t) = H(r)e^{-j\omega t}$$

$$E(r,t) = E(r)e^{-j\omega t} \qquad (2.2)$$

where H(r) and E(r) are the spatial distributions of field contained in a mode of the crystal. These solutions can be plugged into each of the equations in 2.1, resulting in:

$$\nabla . [\varepsilon(r)E(r)] = 0 \qquad \nabla \times E(r) - j\omega\mu_o H(r) = 0$$

$$\nabla . H(r) = 0 \qquad \nabla \times H(r) + j\omega\varepsilon_0 \varepsilon(r)E(r) = 0 \qquad (2.3)$$

The divergence equation on the left side of equation 2.3 shows that the solutions are modes of transverse electromagnetic waves. That is, for plane wave solutions with wave vector k and field component a, a.k = 0. For example, if propagation occurs in the x-direction, the EM components are aligned with a = y or z. The two transverse polarizations primarily considered in this report are the transverse-electric (TE, E orthogonal to k) and transverse-magnetic (TM, H orthogonal to k). Finally, by decoupling the curl equations on the right side of 2.3, substituting for E(r) and remembering that 1/c = $\sqrt{(\varepsilon_o \mu_o)}$, we arrive at the master equation:

$$\nabla \times \left(\frac{1}{\varepsilon(r)} \nabla \times H(r) \right) = \left(\frac{\omega^2}{c^2} \right) H(r) \qquad (2.4)$$

Eqn. 2.4 allows us to directly solve for the states H(r) of a PhC and their eigenvalues in a plane-wave basis, which allows for the plotting of dispersion diagrams for finding bandgaps and resonant modes. The equation is a function of the angular frequency of light ω and the dielectric function in space ε(r). With the master equation in hand, it is important to consider the scalability of Maxwell's equations. The band diagrams which are plotted in this thesis are all normalized to a scale factor usually referred to as 'a'. In PhCs, 'a' is usually set as the lattice constant of the crystal and all other dimensions are defined relative to the lattice constant. Because of this normalization scheme, all eigen value solutions to the master equation are relative to the periodicity of the structure. For example, consider a periodic lattice of holes with hole radius defined as 0.2a; each hole has a relative radius of 1/5 of the lattice spacing. Any solution to the master equation for this lattice thus holds for all PhCs with identical relative lattice dimensions, such as a=500nm, r =100 nm; a=25μm, r =5μm, etc. The free space wavelength of any eigen value solution can then be found by taking the normalized frequency and dividing the real lattice spacing dimension by this value. For instance a calculated normalized mode frequency of ω=0.25a has a wavelength of λ = 500/0.25=2000 nm for a=500 nm.

2.5 SCALING PROPERTIES OF THE MAXWELL EQUATIONS

In case of solid state physics while dealing with electrons one has to define the length scale (e.g. the Bohr radius in atomic physics). But there is no fundamental length scale when it comes to photonic crystals. The master equation is scale invariant. This scaling property is a very powerful feature of electromagnetism in dielectric media. Based on the discussion in previous section, if we have an electromagnetic eigenmode H(r) for frequency ω in a dielectric distribution ε(r), we will have the master equation of H(r):

$$\nabla \times \left(\frac{1}{\varepsilon(r)} \nabla \times H(r)\right) = \left(\frac{\omega^2}{c^2}\right) \mathrm{H(r)} \qquad 2.5$$

Lets define a rescaled dielectric constant ε'(r) = ε(r/s). Now we introduce the variable r' = ar in the master equation and also rescale the Nabla operator accordingly ($\Delta' = \Delta/a$):

$$a\nabla' \times \left(\frac{1}{\varepsilon(r'/a)} a\nabla' \times H(r'/a)\right) = \left(\frac{\omega^2}{c^2}\right) \mathrm{H(r'/a)} \qquad 2.6$$

on dividing equation 2.6 by a^2, we get

$$\nabla' \times \left(\frac{1}{\varepsilon(r'/a)} \nabla' \times H(r'/a) \right) = \left(\frac{\omega^2}{(ac)^2} \right) \text{H(r'/a)} \quad 2.7$$

because ε' (r') = ε' (r'/a)

$$\nabla' \times \left(\frac{1}{\varepsilon'(r')} \nabla' \times H(r'/a) \right) = \left(\frac{\omega^2}{(ac)^2} \right) \text{H(r'/a)} \quad 2.8$$

and after dropping the index in the spatial coordinates, we end up with the known master equation:

$$\nabla \times \left(\frac{1}{\varepsilon'(r)} \nabla \times H(r/a) \right) = \left(\frac{\omega^2}{(ac)^2} \right) \text{H(r/a)} \quad 2.9$$

where the eigen frequency ω and the mode H(r/a) are just rescaled. Hence, we can say that if we know the eigen functions and eigen values for a given length scale, new eigen functions and new eigen values for another length scale can be calculated by simply scaling the old ones.

2.6 PHOTONIC CRYSTAL DEFECTS

The concepts of photonic bandgap materials and photonic crystals have been extensively studied over the recent years. By applying theoretical methods of solid state physics to periodic dielectric structures, the prediction of their properties and behavior is possible. So the dispersion relation of a photonic crystal is a band structure similar to semiconductors.

Structures disturbing the periodicity of the photonic crystal are of special interest, because of their property of acting as guiding or confining elements for light within the crystal. Again, following an analogy to semiconductor crystals that can possess donor and acceptor defect states in the electronic bandgap, the inclusion of PhC defects create states inside the photonic bandgap, which can be utilized to selectively guide light or allow it to resonate in small volumes. If, e.g., a point defect is introduced, defect levels within the photonic bandgap will arise. Their behavior can be donor like or acceptor like, regarding on the type of the defect. While control over the reflectance spectrum of PhCs via the bandgap is useful for applications beyond mirrors (such as in the use of MEMS-based optical scanners), the most interesting applications and devices arise when defects are introduced into the crystal lattice.

Defects can be either a line defect or a point defect. These types of defects are discussed below:

2.6.1 LINE DEFECTS: WAVEGUIDES

Controlling light propagation using PhC line defects [1] differs from classical methods of index guiding, which use total internal reflection to confine light. Index guiding is used in applications of fiber optics and semiconductor planar waveguides when long signal propagation lengths and/or microelectronics process integration are necessary, respectively. The bandwidth of these types of waveguides is determined by the physical dimensions of the waveguide, and discrete modes are supported over a finite range of wavelengths, as governed by the wave equation. Light of wavelengths that are not guided in the structures evanescently decay out of the waveguide. In a photonic crystal waveguide, light is constrained within the linear defect region primarily because it is not supported elsewhere; it is essentially trapped in the waveguide region. This is most evident in the rod PCS, where line defect waveguides can even guide light in regions of air. In hole PCS structures, waveguides are formed by filling in one row of holes in the Γ-K direction as shown in Fig. 2.7. Light with the same momentum (frequency) as that of the defect state can propagate in the linear defect, and when only a single mode exists propagation occurs with very low-loss.

The nomenclature of different waveguide types follows the number of rows removed in the defect: a “W1” waveguide has one row removed, while a “W2” has two rows missing. Adding more rows to a waveguide adds more guiding bands within the gap, whereas shrinking the waveguide width creates wider bandwidth guiding bands.

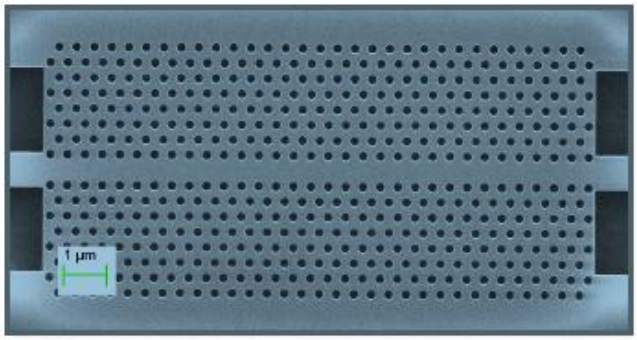

Figure 2.7: Fabricated photonic crystal W1 waveguide and input/output strip waveguides, formed by a single line defect

[Image Source: Multiple-hole defects: optimizing light-matter interaction in photonic crystal cavities by Christopher Kang]

2.6.2 POINT DEFECTS: RESONATORS

When the properties of one or more lattice points are modified, an isolated region of broken symmetry is created, surrounded by the periodic PhC lattice. For example, the radius of one lattice hole can be modified, making it smaller or larger relative to the surrounding lattice holes (a "single-hole defect", SHD), or by filling in the hole altogether. Point defects are commonly named according to their symmetry and dimensions: single filled-in holes are named "H1" defects due to their hexagonal symmetry, and filling in more holes results in a "L2," "L3," etc (due to their linear fashion). Examples of these defects are illustrated in Fig. 2.8.

The broken symmetry creates a resonant state within the bandgap, the frequency of which is the characteristic resonance frequency of light associated with the cavity geometry.

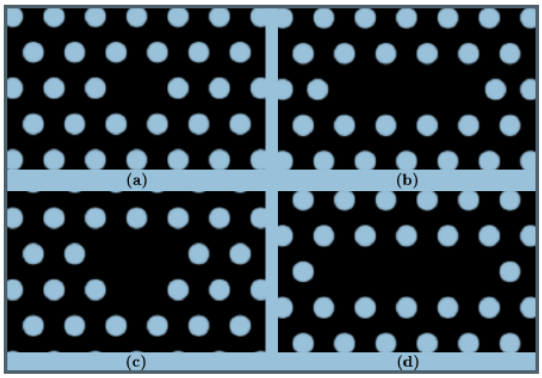

Figure 2.8: Different types of PhC cavities: (a) H1, (b) L3, (c) T3, (d) L4 type.

Source: Multiple-hole defects: optimizing light-matter interaction in photonic crystal cavities by Christopher Kang

At resonance, photons are trapped inside the cavity for some time period until they are eventually lost by leakage, absorption, or scattering. The time constant't' associated with the photon energy decay in the cavity is directly related to a measurable quantity called "quality factor," commonly referred to as Q [7, 8]. Q depends on the decay time constant and the full-width half maximum (FWHM) of the resonance peak in the transmission. The longer light resonates inside the cavity, the higher the quality factor. A small FWHM (figure 2.9) gives a narrower resonance and a higher Q. Q can be define as in equation 2.10, where

$$Q=\omega_0/\Delta\omega_{1/2} = \lambda_0 /\Delta\lambda_{1/2} \quad (2.10)$$

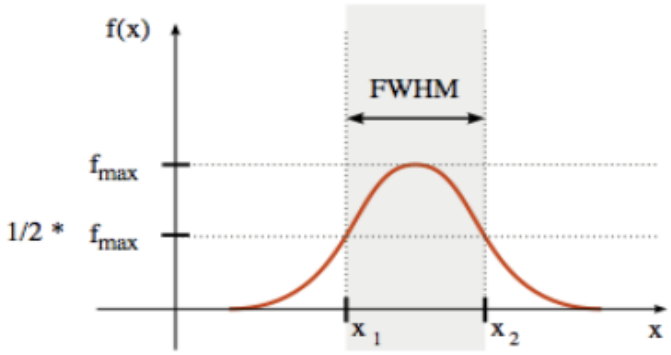

Figure 2.9: Full-Width at Half Maximum for a cavity resonance.

2.7 INTRODUCTION TO THE SOFTWARE AND METHOD USED

R-Soft (2011) is commercially available software that includes many modules. Namely, BandSolve module allows one to compute the band structures of the PhC as well as its modes' field distribution by means of PWE method while Fullwave implements FDTD method applying it to the field distribution computation inside the arbitrary structures and, in special case, the band structure.

2.7.1 PLANE WAVE EXPANSION

Plane wave expansion (PWE) is a frequency-domain computational method which can be used to directly solve for eigenstates of the master equation (Eqn. 2.4). The bandgap of the photonic crystal can then be found by plotting the band diagram, using the calculated eigenvalues of the modes.

The iterative method uses a pseudo-random field to initiate the eigensolver, and the modes are solved over a spatial grid determined by the resolution parameter, until good agreement with a preset convergence factor is reached. The resolution in this case is defined as the number of points per lattice constant 'a'. For the 2D photonic crystal, which is periodic only in the plane of propagation, the periodic boundary condition holds for the x and y-directions of the supercell illustrated in figure 2.10.

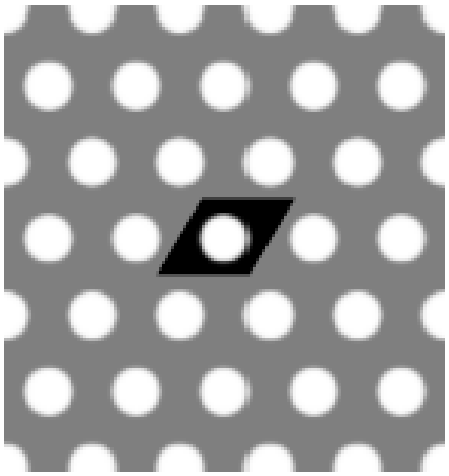

Figure 2.10: The photonic crystal dielectric function highlighting the unit cell of interest in the hexagonal basis

The periodic boundary condition generally repeats the super cell in all dimensions according to the specified basis vectors. For the case of the hexagonal lattice, the basis vectors are specified as, $\left(\frac{1}{2}, -\frac{\sqrt{3}}{2}\right)$ and $\left(\frac{1}{2}, \frac{\sqrt{3}}{2}\right)$.

2.7.2 FINITE-DIFFERENCE TIME-DOMAIN

Finite-difference time-domain (FDTD) analysis is a numerical, time-domain method of examining the propagation of electromagnetic fields by solving Maxwell's equation in dielectric structures. The desired dielectric structures and dipole sources are placed inside a spatially-gridded 'cell' and the fields are iterated in time by calculating the electric and magnetic field over all grid points. In time-domain calculations, Fourier analysis enables the frequency response of structures to be computed by using a source with a broadband frequency component (a short pulse in time). The 'Fullwave' module of 'R-Soft' software was used for FDTD calculations, which supports sub pixel averaging of dielectric interfaces for increased accuracy. ε-averaging improves the modeling of high contrast dielectric interfaces by averaging features when they cannot be clearly resolved by the set resolution.

CHAPTER 3

INTRODUCTION TO OPTICAL LOGIC GATES

3.1 INTRODUCTION

Communication based on internet has become an order of the day with the ever-expanding user base. The requirements have besieged the available bandwidths and higher speeds have now become mandatory to satisfy the user's demands and thus increasing as well as sustaining the use of internet. Integrated circuits and electronic devices could cope with the ever increasing requirement of high speed data transmission and also processing with the help of innovations in microelectronics. As per the Moore's Law the electronic processor speed doubles roughly every 18 months nevertheless it comes at the cost of increased chip power consumption and the dissipation. Hence, a novel innovation way-out to this problem is needed and the photonic devices are one of the promising solutions in this horizon.

An optical component permits the miniaturization of photonic integrated circuits to a scale comparable to the wavelength of light and thus proves to be good candidates for future optical network and optical computing. All-optical communication is one among the solutions for electronic bottleneck viz size and speed, as optical devices are able to process the information at the speed of light. In the past years researchers have demonstrated all-optical logic gates using different schemes based on nonlinear effects in optical fibers, in semiconductor devices and in waveguides. But most of the reported works suffer from certain fundamental limitations including low speed, big size and difficult to perform chip-scale integration.

At the present time PhC are drawing significant attention as a platform on which devices with dimensions in the order of wavelengths of light for future photonic integrated circuits can be built. PhC have some very unique properties such as high speed, low power consumption, compactness, better confinement and tailoring dispersion which makes them promising candidate in photonic integrated circuits.

Basically the physical medium which carries light from one place to the other in optical domain provides a large bandwidth. Optical devices that are computing in optical domain namely optical processor which consists of photonic logic gates and optical integrated circuits are highly envisaged

as an alternate feasible and they can also provide the standard shift from the extreme short comes imposed on the speed and also on the complexity of the present day processing by the conventional electronics.

As already discussed, photonic crystals have brought a significant reformation to the photonic and optical device designing in the past years.

Recently, all-optical logic gates have been attracting extensive attention because of their applications in the fields of optical computing systems and optical interconnection networks. Many schemes have been proposed to realize all-optical logic gates, including the use of nematic liquid crystals [23], metallic (or dielectric) waveguides [24–26], and silicon optical resonators [27]. Because of their exceptional ability to control the propagation states of photons, photonic crystals, with their photonic bandgaps, are considered as one of the most suitable candidates for the realization of integrated photonic devices. All-optical logic gates based on photonic crystals are capable for practical on-chip applications. Photonic crystal-based all-optical logic gates can be realized through interferometer [28], Mach-Zehnder interferometer (MZI) [29] and semiconductor optical amplifier (SOA) [30] and nonlinear processes including electro-optical effect [31, 32], thermal-optical effect [33] and two-photon absorption [34].

3.2 COMPARISON BETWEEN ELECTRONIC LOGIC GATES AND ALL-OPTICAL LOGIC GATES

Logic gates are the devices that perform a certain Boolean logic operation on one or more logical inputs and produce a single logical output. Boolean algebra generally comprises of operations that give “true” or “false” as a result. In this lies the foundation of digital electronics and computing. It is standard to express true and false as 1 and 0, respectively. Logic gates are bistable devices, that is, they may yield either of these two possible stable outputs. It is common to see ‘1’ corresponding to 5 Volts and ‘0’ corresponding to 0 Volts in digital electronics. The relationship between input and output signals are displayed in what are known as truth tables.

These Boolean logic devices are not limited to electronics only. They have also been demonstrated with optics in many different implementations with various switching mechanisms. The optical version of these logic gates is grabbing more interest because the conventional computational

speeds are approaching limits. Also the miniaturization attempts in lithography (in an attempt to fit as many transistors as possible on a single chip) are becoming problematic.

Optical computing can have many advantages over electronic computing. Some examples include:

- Immunity to electronic interference
- Lighter, more compact systems
- Immunity to short circuits
- Lower-loss transmission
- Significantly more bandwidth
- Easier/cheaper parallel computing

To sum up we can say a logic gate is an elementary building block of any circuit and have two or more inputs and one output. Logic levels i.e. 0 or 1 in binary logic system are physically represented by signal levels, which may be either voltage or current in electronics circuits. In case of optical circuits, logic levels are represented by signal intensity / phase / polarization, and are differentiated by different threshold.

Digital data can be transmitted to electronic processors through an optical fiber with speed of light, but maximum speed of switching of electronic logic gates is 50ps for the average power 0.5mW (energy of fJ) per switching (1995). It is also known that the switching speed of logic gates based on semiconductors is generally restricted by the capacitance of the p-n junctions. Even though the size of the modern semiconductor logic gates is small, their switching is limited by the interlinking capacitance. Also at the same time, the switching speed of the optical logic gates is in Femto second range (Yavuz 2006) and is limited only by velocity of light passing through it. By this it means that optical switches may switch data approximately 1000 times faster than their electronic counterparts. Photons with different wavelength can travel together in the same fiber or cross each other in the free space without any interference or cross-talk. This enables the possibility of parallelism in the optical processing. Generally optics provides higher bandwidth than electronics, which in turn enables more of the information to be carried out simultaneously and the ease of the data to be processed in parallel without any interference. The optical signal processing is immune to electromagnetic interference and free from electrical short circuits.

Consequently in the developing of a family of optical logic devices with the Boolean functionality, an optical equivalent of the Transistor-Transistor Logic (TTL) is an important step in this direction.

3.3 APPLICATION OF ALL-OPTICAL LOGIC GATES

All-optical logic gates can perform many logic functions. They find numerous applications in optical communication, optical signal processors, optical network, optical instrumentation, etc.

All-optical AND gate serves as a sampling gate in optical sampling oscilloscopes. It can perform address recognition, data-integrity verification, optical header recognition and wavelength converter. All- optical NOT gates can be used as an inverter, Manchester encoded signal generator and as a switch.

All-optical XOR gate is very important in the decision and comparator circuits. It also performs a different set of processing functions, including the comparison of data patterns for the address recognition and packet switching, bit-serial parity checking, data encryption and decryption label swapping, etc.

NOR gate is then utilized for monitoring the error detection, address and the header recognition, data encoding, encryption, etc.

The XNOR gates are applied in pattern-matching module that produces output pulse for all bits that do match and find the missing pulses at output.

Combinations of optical logic gates are employed to perform the basic or complex computing and the arithmetic functions such as binary subtraction, addition, encoding, decoding and are even used to build binary counter, flip-flops and Random Access Memory Cell.

Out of all these optical logic gates NAND and NOR are the universal gates and rest all are the basic gates. Universal optical gates are the ones that can implement any Boolean function without the need to use any other optical logic gate types and also all the other optical logic gates can be implemented using the combination of universal optical logic gates. In practice, it is advantageous since NAND and NOR gates are economical and easier to fabricate. Thus, we have tried to design all the basic optical logic gates using the combination of all-optical NAND gates.

CHAPTER 4

DESIGN OF ALL THE OPTICAL LOGIC GATES USING UNIVERSAL NAND GATE

4.1 INTRODUCTION

In this thesis, we have proposed the design of all-optical logic gates using the combination of universal NAND gates. A universal gate is a gate which can implement any Boolean function without need to use any other gate type. The NAND and NOR gates are universal gates. In practice, this is advantageous since NAND and NOR gates are economical and easier to fabricate and are the basic gates used in all logic families. Initially, optical NAND gate has been designed and optimized. Further, three similar optical NAND gates have been arranged in such a manner that the combination will work as optical AND, OR, XOR and XNOR gates. Each time the inputs vary according to the basic optical gate to be designed. The optical XOR and XNOR gates are designed using this three optical NAND gate combination, when the complemented inputs are available prior hand. This complemented input can be obtained using an inverter or an optical NOT gate. The proposed optical logic gate combination is based on the phenomenon of optical interference effect and is designed on two dimensional photonic crystal wave-guides composed of air holes in silicon. When the power of light obtained at the output port is more than 50% of the power fed at the input ports, logic 1 is considered else logic 0. The simulation results show that the proposed optical photonic crystal waveguide structure could really function as optical logic all-optical AND, OR, NOT, XOR and XNOR logic gates.

4.2 DESIGN AND OPERATING PRINCIPLE OF ALL-OPTICAL LOGIC NAND GATE

In this thesis work, the proposed two dimensional (2D) photonic crystal structure, consists of triangular lattice of air holes (refractive index n=1) in silicon having refractive index n = 3.5. The layout used to design the NAND gate has been taken as 45 by 45 air holes in silicon background. The radius (r) of air holes is 0.3a, where, ‘a’ is the lattice constant equal to 0.352 μm. In the photonic crystal structure composed of air holes in dielectric, only TE polarization exists. The first band gap lies in the normalized frequency region ($\omega a / 2\pi c$) 0.206 to 0.274 as shown in figure 4.1.

The photonic band diagram of the bulk PhC shows that the light with wavelength range of 1.2848-1.7017 μm for TE modes cannot pass through the uniform PhC structure.

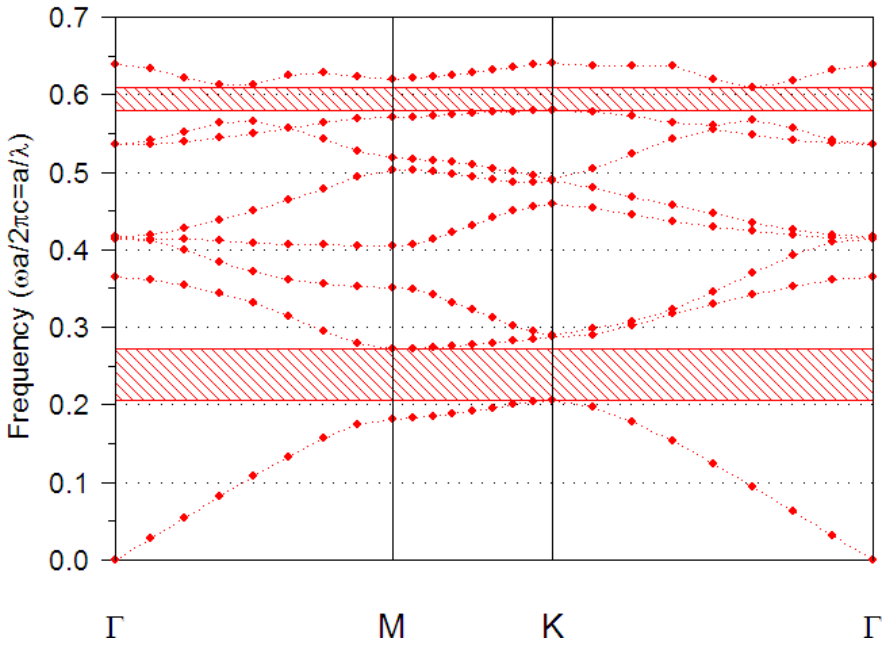

Figure 4.1: Band gap of the Photonic crystal structure composed of r=0.3a.

To design the basic NAND gate design four waveguides have been created, out of which two of them are considered as input ports indicated as port A and port B. One port has been indicated as reference port R which is used to create phase difference between the input signals resulting into either constructive or destructive interference. Output signals of NAND gate are obtained from the right port indicated as output port Y as shown in figure 4.2. Further, in the proposed structure a hole has been introduced at the center of the four waveguides and six holes have been placed at the outer edge of the waveguide (port A and port B). Size and location of the holes at the edge are optimized such that there are minimum bend losses. For the design of all optical logic gates the radius of the central hole is optimized in such a way that when a single input in phase with reference signal is launched gives the maximum power ; and when both the inputs out of phase with the reference signal is launched gives the minimum power at the output port Y.

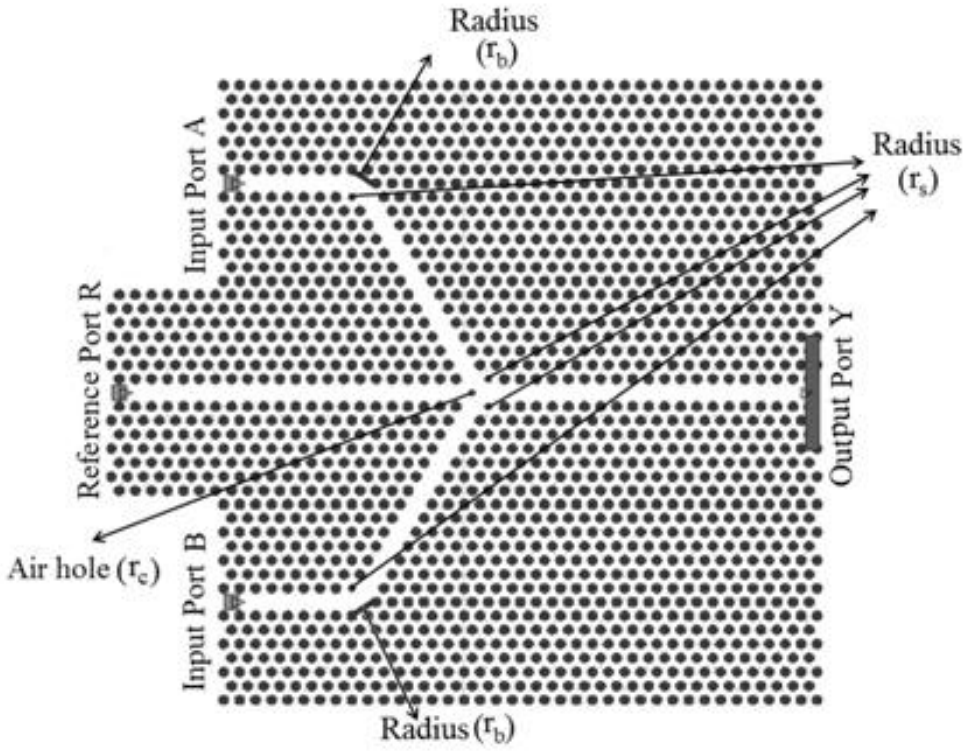

Figure 42: Layout of optical logic NAND gate

4.3 OPTIMIZATION OF NAND GATE

The radius of the hole placed in the center of the four waveguides, has been optimized when one of the input signals is in phase with the reference signal; and both the input signals are out of phase with the reference signal. As the radius of the central hole increases, the output power increases to maximum value and decreases to a minimum value for single input signal and in the case when both the input signals are out of phase with the reference then the output power increases for both the input signals as shown in figure 4.3. Hence the radius of the center hole is taken to be 0.2a. To reduce the bending losses in the NAND gate six air holes of radius r_b = 0.15a have been placed at outer bend edge of the input waveguide and radius of the inner edge air hole (r_s) has been reduced to 0.17a.

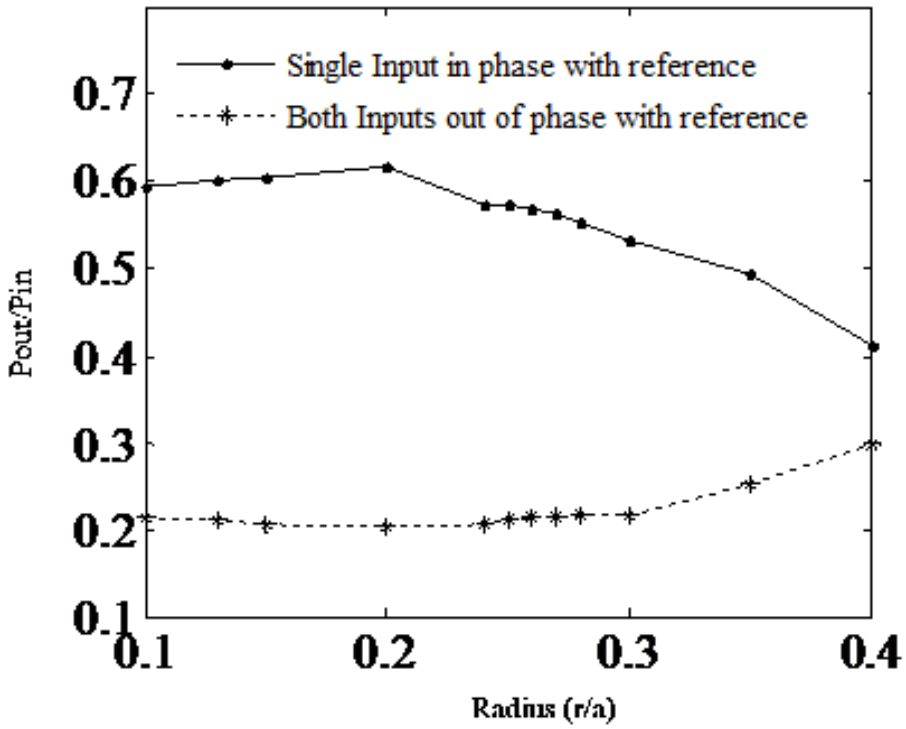

Figure 4.3: Variation of the normalized output power with the radius of the central air hole

4.4 SIMULATION AND RESULTS OF NAND LOGIC GATE

After the optimization of the basic NAND gate structure the logic operation has been performed using finite difference time domain method. The logic operation has been explained as follows:

(i) When only the reference signal has been applied and none of the input ports have been excited with the continuous wave source then logic '1' is obtained at the output port.

(ii) When either of the input ports have been excited with the input signal along with the reference signal in phase with each other then also logic '1' is obtained at the output port Y.

(iii) When both the input ports have been excited simultaneously and is out of phase with the reference signal then logic '0' is obtained at the output port Y.

When the output power at the output port Y is less than 0.5 P, it has been considered as logic 0 or otherwise logic 1. The simulation results summarized in table 1 and field distributions shown in figure 4.4 clearly indicate that the proposed structure works as NAND optical logic gate.

A single NAND gate can behave as optical NOT gate as has been summarized in table 2.

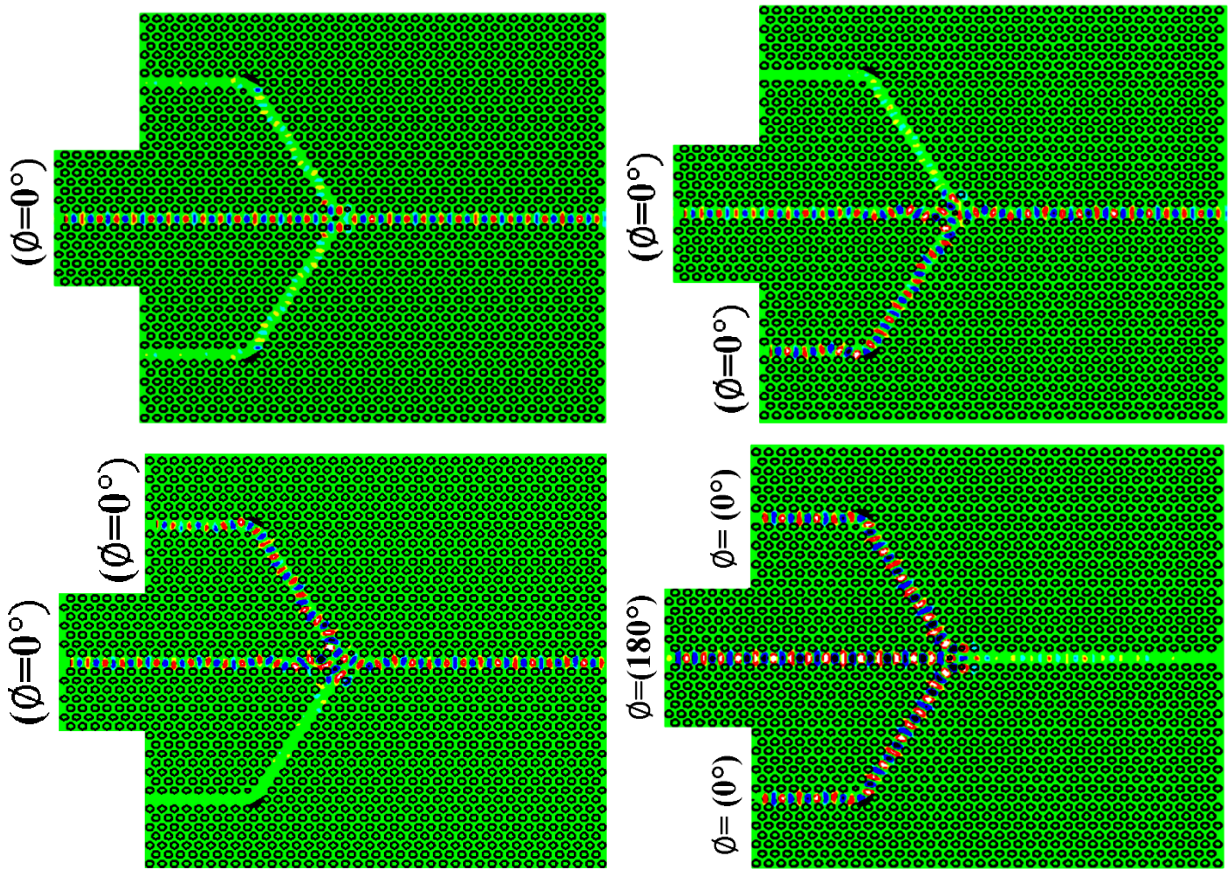

Figure 4.4: NAND gate field distributions for (a) A=0, B=0 and R=1, (b) A=0, B=1 and R=1 (c) A=1, B=0 and R=1 (d) A=1, B=1 and R=1

Table 1: Truth table for NAND logic gate where output Y is in terms of input power P

Input A (Ø=0°)	Input B (Ø=0°)	Reference signal (R)	Logic output	Normalized Output Y
0	0	1(Ø=0°)	1	0.825 P
0	1	1(Ø=0°)	1	0.705 P
1	0	1(Ø=0°)	1	0.700 P
1	1	1(Ø=180°)	0	0.250 P

Table 2: Truth table for NOT logic gate where output Y is in terms of input power P

Input A (Ø=0°)	Input B (Ø=0°)	Reference signal (R)	Logic output	Normalized Output Y
0	0	1(Ø=0°)	1	0.850 P
1	1	1(Ø=180°)	0	0.250 P

4.5 DESIGN AND SIMULATION OF BASIC GATES USING NAND GATE

The proposed combination structure comprising of three optical NAND gates is a two dimensional (2D) photonic crystal structure that consists of triangular lattice of air holes (refractive index n=1) in silicon having refractive index n = 3.5. The layout used to design the basic gates using the optical NAND gate has 110 by 110 air holes in silicon background. The radius (r) of air holes is 0.3a, where 'a' is the lattice constant equal to 0.352 μm.

The structure has three optical NAND gates. These three gates are placed in a manner that output from two becomes the input to the other. The output Y from the third NAND gate is the final input. The concept used for designing and simulation is that when the light is launched with power P from the input ports and if the output power is less than 50% of P, it will be a logic 0 otherwise a logic 1. All the other optical logic gates including AND, OR, XOR and XNOR are designed using the same combination of three and are discussed as follows.

4.5.1 AND gate

Firstly, the function of optical logic AND gate has been demonstrated. In the combined structure each NAND gate composed of two input signals, one reference signal and one output signal. Reference signal R and input signals A and B have been introduced into the NAND gate1 and NAND gate 2 and their output Y1 and Y2 respectively along with the reference signal R' serve as the input signals for the NAND gate 3 and output Y is the final output for the AND gate as shown in figure 4.5. The AND logic gate works as follows:

(i) When none of the input ports (port A and port B) have been excited and only the reference port R having phase angle ∅=0°, and reference port R' having phase angle ∅=180° have been excited then logic 0 is obtained at the output port Y.

(ii) When either of the input ports i.e. input port A or input port B have been excited with light having phase angle ∅=0°, along with the reference port R with light having phase angle ∅=0°, and port R' having phase angle ∅=180° then also logic 0 is obtained at the output port Y.

(iii) When both the input ports A and B have been excited with light signal having phase angle ∅=0°, along with the reference port R with phase angle ∅=180° and port R' having phase angle ∅=0°, then logic 1 is obtained at the output port Y.

The results have been summarized in table 3.

4.5.2 OR gate

For OR gate the output is '0' if and only if both the input values are 0 otherwise output values are 1. The OR gate design using combination of NAND gates have slight variations from the AND gate. The input A have been considered for the NAND gate 1 and input B have been considered for NAND gate 2 as shown in figure 4.6. The function of optical logic OR gate using the combination of NAND gates have been demonstrated as follows:

(i) When only input port A have been excited with light having phase angle ∅=0°, along with the reference port R with light having phase angle ∅=0°, and reference port R' also having phase ∅=0°, then logic 1 is obtained at the output port Y.

(ii) Similarly, when only input port B have been excited with light having phase angle ∅=0°, along with the reference port R with light having phase angle ∅=0°, and reference port R' also having phase angle ∅=0°, then logic 1 is obtained at the output port Y.

(iii) When both the input ports A and B have been excited with light signal having phase angle∅=0°, reference port R with light having phase angle ∅=180° and port R' having phase ∅=0°, then logic 1 is obtained at the output port Y.

(iv) When no signal have been launched at input ports A and B, but excited with reference signal R having phase angle ∅=0°, and reference signal R' having phase angle∅=180° then logic 0 is obtained at the output Y.

The results have been summarized in table 4.

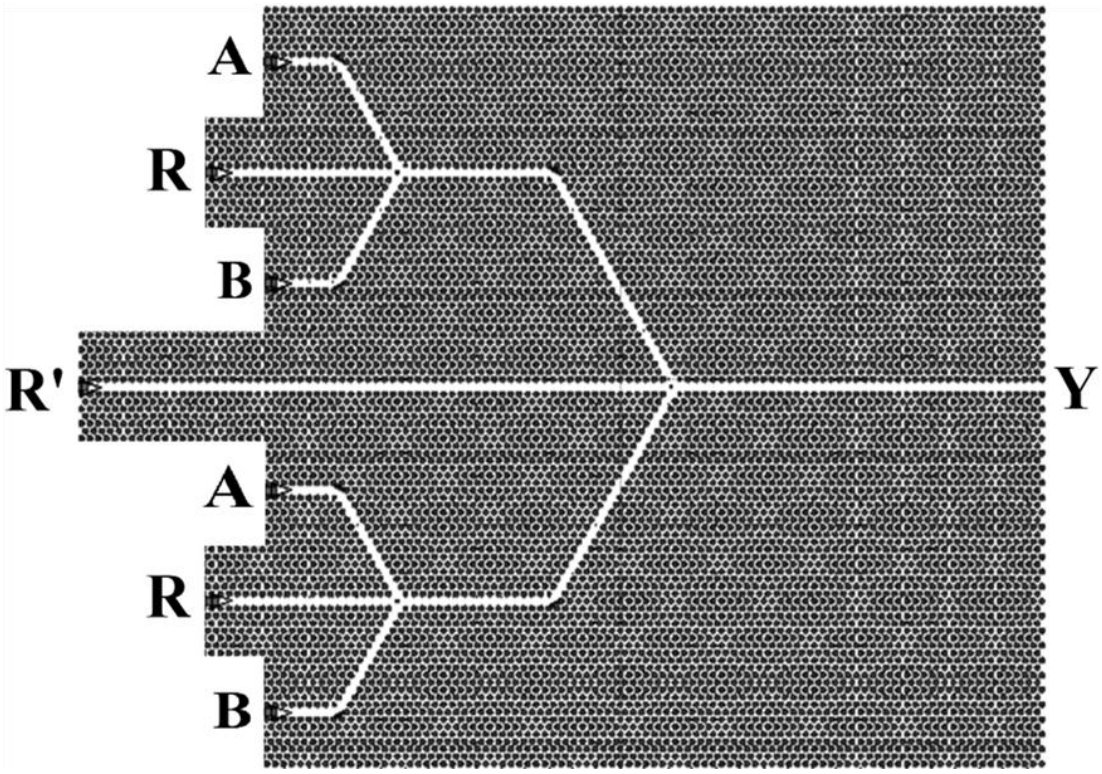

Figure 4.5: Optical logic AND gate layout using three NAND gates

Table 3: Truth table for AND logic gate where output Y is in terms of input power P

Input A (Ø=0°)	Input B (Ø=0°)	Reference signal (R)	Reference signal (R')	Logic output	Normalized Output Y
0	0	1(Ø=0°)	1(Ø=180°)	0	0.06 P
0	1	1(Ø=0°)	1(Ø=180°)	0	0.150 P
1	0	1(Ø=0°)	1(Ø=180°)	0	0.150 P
1	1	1(Ø=180°)	1(Ø=0°)	1	0.950 P

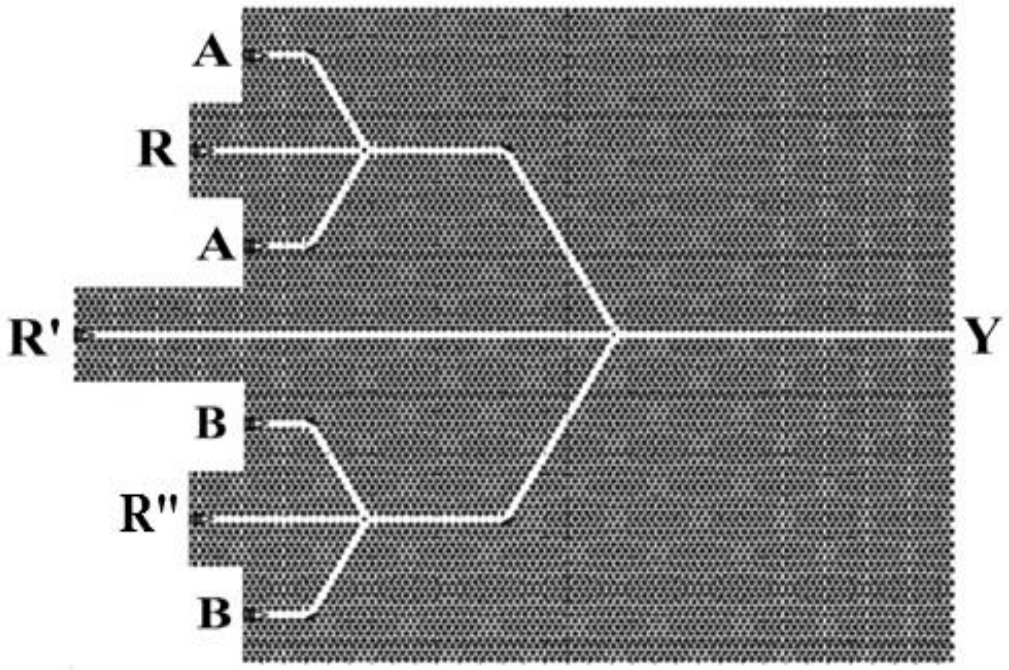

Figure 4.6 Optical logic OR gate layout using three NAND gates

Table 4: Truth table for OR logic gate where output Y is in terms of input power P

Input A (Ø=0°)	Input B (Ø=0°)	Reference signal (R)	Reference signal (R")	Reference signal (R')	Logic output	Normalized Output Y
0	0	1(Ø=0°)	1($_{\phi}$=0°)	1(Ø=180°)	0	0.051 P
0	1	1(Ø=0°)	1($_{\phi}$=180°)	1(Ø=0°)	1	0.904 P
1	0	1(Ø=0°)	1($_{\phi}$=0°)	1(Ø=0°)	1	0.891 P
1	1	1(Ø=180°)	1($_{\phi}$=180°)	1(Ø=0°)	1	0.717P

4.5.3 XOR gate

In XOR logic gate output is logically high (1) if one, and only one of the two inputs to the logic gate is high (1) and logically low (0) if both the inputs are high or low. When the complement of inputs A and B are available, XOR gate can be designed by using combination of three NAND gates. The design of XOR gate using three NAND gates has been shown in the figure 4.7. Each NAND gate has two input ports, one reference port and one output port.

The working of XOR logic gate using the proposed combined structure has been explained as follows:

CASE (i)

When both the inputs A and B are low and complements of A and B are available:

For the NAND gate 1 when the input port C which is the complemented form of input A is launched with light having phase angle ∅=0° along with reference port R_1 with light having phase angle ∅=0° then logic 1 is obtained at the output Y1. Similarly, for the NAND gate2 when the input port D which is the complemented form of input B is launched with the light having phase angle ∅=0° along with reference port R_2 with light having phase angle ∅=0° then logic 1 is obtained at the output Y2. Output Y1 and Y2 as the inputs signals for the NAND gate 3 along with the reference port R' launched with the light having the phase angle ∅=180° gives logic 0 at the output port Y.

CASE (ii)

When the input A is low and B is high and complements of A and B are available:

For the NAND gate 1 when the input port C which is the complemented form of input A and input port B are launched with light having phase angle ∅=0° along with reference port R_1 with light having phase angle ∅=180° then logic 0 is obtained at the output Y1. Similarly, for the NAND gate2 when the reference port R_2 is launched with light having phase angle ∅=0° then logic 1 is obtained at the output Y2. Output Y1 and Y2 as the inputs signals for the NAND gate 3 along with the reference port R' launched with the light having the phase angle ∅=0° gives logic 1 at the output port Y.

CASE (iii)

When the input A is high and B is low and complements of A and B are available:

For the NAND gate1 when the reference port R_1 is launched with light having phase angle ∅=0° then logic 1 is obtained at the output Y1. For the NAND gate2 when the input port D which is the

complemented form of input B and input port A are launched with the light having phase angle ∅=180° along with reference port R_2 with light having phase angle ∅=0° then logic 0 is obtained at the output Y2. Output Y1 and Y2 as the inputs signals for the NAND gate 3 along with the reference port R' launched with the light having the phase angle ∅=0° gives logic 1 at the output port Y.

CASE (iv)

When both the inputs A and B are high and complements of A and B are available:

For the NAND gate 1 when the input port B is launched with light having phase angle ∅=0° along with reference port R_1 with light having phase angle ∅=0° then logic 1 is obtained at the output Y1. Similarly, for the NAND gate2 when the input port A is launched with the light having phase angle ∅=0° along with reference port R_2 with light having phase angle ∅=0° then logic 1 is obtained at the output Y2. Output Y1 and Y2 as the inputs signals for the NAND gate 3 along with the reference port R' launched with the light having the phase angle ∅=180° gives logic 0 at the output port Y. The results are summarized in table 5.

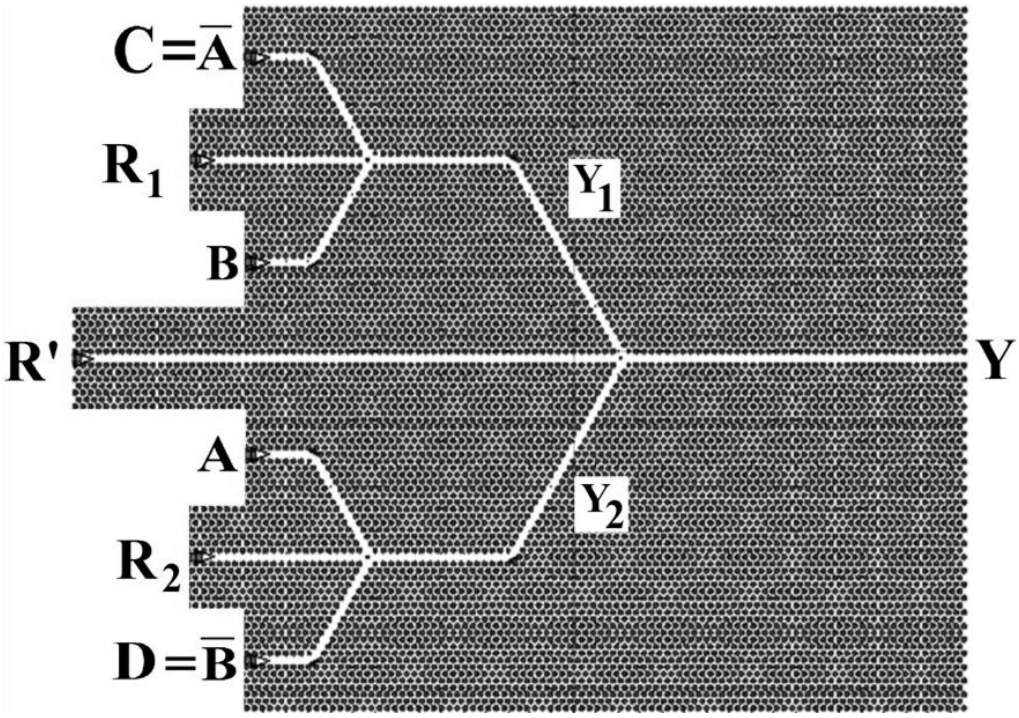

Figure 4.7 Optical logic XOR gate layout using three NAND gates

Table 5: Truth table for XOR logic gate where output Y is in terms of input power P

Input A (Ø=0°)	Input B (Ø=0°)	Input C (complement of A) (Ø=0°)	Input D (complement of B) (Ø=0°)	Reference signal(R_1)	Reference signal(R_2)	Reference signal (R')	Logic Output	Normalized Output Y
0	0	1	1	1(Ø=0°)	1(Ø=0°)	1(Ø=180°)	0	0.150 P
0	1	1	0	1(Ø=180°)	1(Ø=0°)	1(Ø=0°)	1	0.575 P
1	0	0	1	1(Ø=0°)	1(Ø=180°)	1(Ø=0°)	1	0.560 P
1	1	0	0	1(Ø=0°)	1(Ø=0°)	1(Ø=180°)	0	0.160

4.5.4 XNOR gate

XNOR logic gate is logical complement of XOR gate. A high (1) output is obtained if both of the inputs are same. It gives logic 0 if one but not both inputs are logic 0. When the complement of inputs A and B are available, XNOR gate can be designed by using combination of three NAND gates. The design of XNOR gate using three NAND gates has been shown in the figure 4.8. Each NAND gate has two input ports, one reference port and one output port.

The working of XNOR logic gate using the proposed combined structure has been explained as follows:

CASE (i)

When both the inputs A and B are low and complements of A and B are available:

For the NAND gate 1 when the reference port R_1 is launched with light having phase angle Ø=0° then logic 1 is obtained at the output Y1. Similarly, for the NAND gate2 when the input port C and D which are the complemented form of input A and B respectively are launched with the light having phase angle Ø=0° along with reference port R_2 with light having phase angle Ø=180° then logic 0 is obtained at the output Y2. Output Y1 and Y2 as the input signals for the NAND gate 3 along with the reference port R' launched with the light having the phase angle Ø=0° gives logic 1 at the output port Y.

CASE (ii)

When the input A is low and B is high and complements of A and B are available:

For the NAND gate 1 when the input port B is launched with light having phase angle ∅=0° along with reference port R_1 with light having phase angle ∅=0° then logic 1 is obtained at the output Y1. Similarly, for the NAND gate2 when the input port C which is the complemented form of A along with the reference port R_2 is launched with light having phase angle ∅=0° then logic 1 is obtained at the output Y2. Output Y1 and Y2 as the inputs signals for the NAND gate 3 along with the reference port R' launched with the light having the phase angle ∅=180° gives logic 0 at the output port Y.

CASE (iii) when the input A is high and B is low and complements of A and B are available:

For the NAND gate1 when the input port A along with the reference port R_1 is launched with light having phase angle ∅=0° then logic 1 is obtained at the output Y1. For the NAND gate2 when the input port D which is the complemented form of input B is launched with the light having phase angle ∅=0° along with reference port R_2 with light having phase angle ∅=0° then logic 1 is obtained at the output Y2. Output Y1 and Y2 as the inputs signals for the NAND gate 3 along with the reference port R' launched with the light having the phase angle ∅=180° gives logic 0 at the output port Y.

CASE (iv)

When both the inputs A and B are high and complements of A and B are available:

For the NAND gate 1 when the input port A and B are launched with light having phase angle ∅=0° along with reference port R_1 with light having phase angle ∅=180° then logic 0 is obtained at the output Y1. Similarly, for the NAND gate2 when the reference port R_2 with light having phase angle ∅=0° then logic 1 is obtained at the output Y2. Output Y1 and Y2 as the input signals for the NAND gate 3 along with the reference port R' launched with the light having the phase angle ∅=0° gives logic 1 at the output port Y. The results are summarized in table 6.

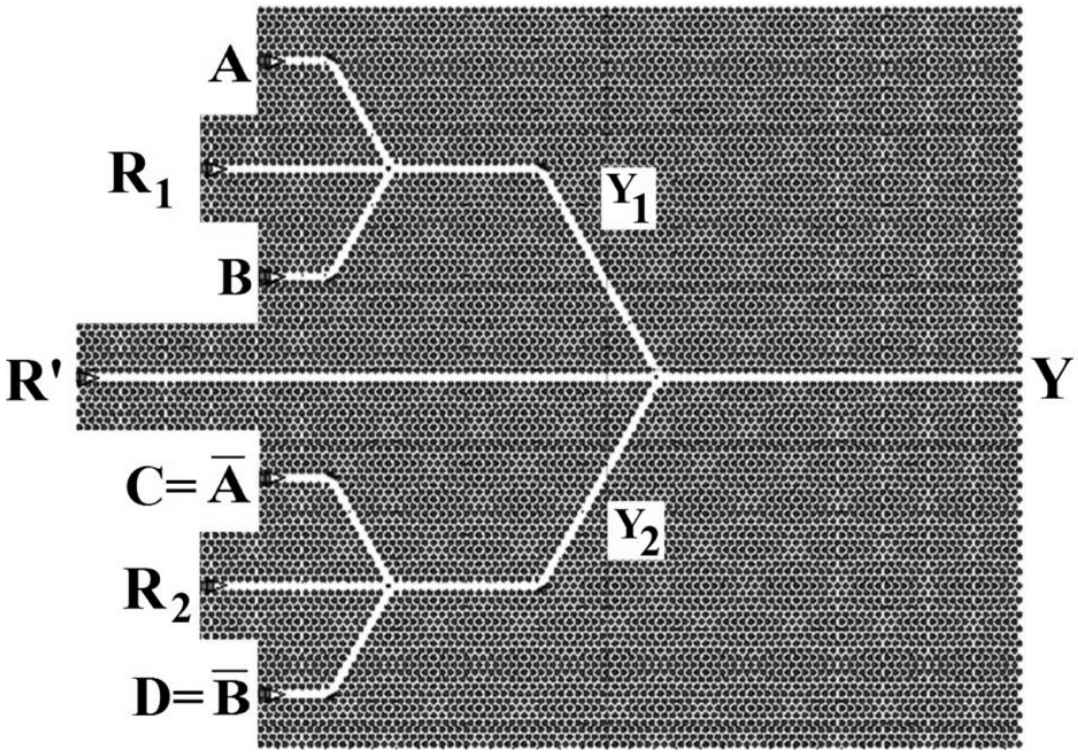

Figure 4.8 Optical logic XNOR gate layout using three NAND gates

Table 6 Truth table for XNOR logic gate where output Y is in terms of input power P

Input A (Ø=0°)	Input B (Ø=0°)	Input C (complement of A) (Ø=0°)	Input D (complement of B) (Ø=0°)	Reference signal(R_1)	Reference signal(R_2)	Reference signal (R')	Logic Output	Normalized Output Y
0	0	1	1	1(Ø=0°)	1(Ø=180°)	1(Ø=0°)	1	0.560 P
0	1	1	0	1(Ø=0°)	1(Ø=0°)	1(Ø=180°)	0	0.160 P
1	0	0	1	1(Ø=0°)	1(Ø=0°)	1(Ø=180°)	0	0.150 P
1	1	0	0	1(Ø=180°)	1(Ø=0°)	1(Ø=0°)	1	0.575 P

4.6 RESPONSE TIME

Response time is defined as the time taken by a system or unit to react to a given input. Response time is thus, the total amount of time a system takes to respond to a request. The figure 4.9 showing the time response of the proposed combined structure concludes that the time taken by the output power to reach from 0 to 90% of the output power in final steady state is ct= 277.4 μm or t=3.23 ps and it consists of two parts out of which one is the time due to transmission delay i.e. t_1=1.615 ps and another t_2= 1.621 ps is the time for the power at the output to reach 0.1% of the maximum power. As the structure is based on linear material it is can be expected that the falling time will be approximately equal to t_2 i.e. 1.621 ps. Thus a narrow pulse of width $2t_2$=3.242 ps can be produced and response time will be 6.48 ps and finally the bit rate will be 0.15 Tb/sec.

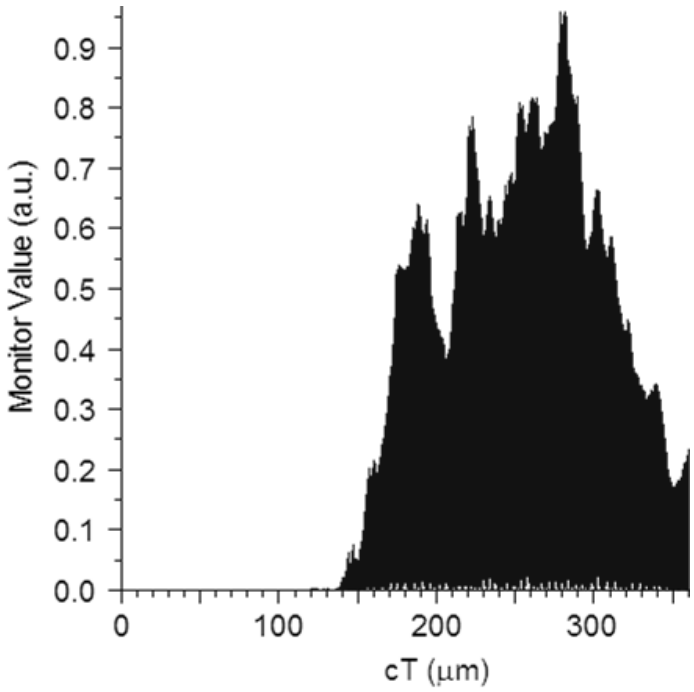

Figure 4.9 Output power used for the calculation of response time

4.7 RESULT

In this thesis, we have proposed the design of all-optical logic gate using the combination of universal NAND gates in two-dimensional PhC waveguides. The optimized optical NAND gate when arranged in a combination of three optical NAND gates and proper inputs are fed at the input ports, the desired logic results are obtained at the output port. The power greater than 50% of P is taken as logic 1 and less than 50% of P is taken as logic 0. Also the response time and the bit rate of

the combined structure are calculated, which are 6.48ps and 0.154 Tb/sec respectively. Since universal gates are cost effective, this thesis work can turn out to be good for the optical computing and photonic integrated circuits.

CHAPTER 5
CONCLUSION AND FUTURE SCOPE

5.1 CONCLUSION

In this thesis, we endeavor to further understand the guidance of light in photonic crystal waveguide and thus have proposed the design for all the optical logic gates including AND, OR, NOT, XOR and XNOR gate, using the combination of three universal all-optical NAND gate in two dimensional photonic crystal waveguides. This thesis work shows that by setting the appropriate path difference, the required interference can be created at the junction point of all the port of the gate.

The performance of the proposed PhC structure has been analyzed by PWE method. Transmission and optimization characteristics have been obtained using FDTD method.

Initially, a single NAND gate with two input ports, one reference port and one output port has been optimized by placing an air hole at the junction of these four waveguides. Further optimization has been done at the bends of the NAND gate so as to minimize the bending losses. The optimized optical NAND gate is further arranged in a combination of three so that the resultant designed structure behaves as the optical logic gates fed with their respective inputs. This cascaded structure has a response period of 6.48ps and bit rate of 0.154 Tb/sec.

5.2 FUTURE SCOPE OF THE WORK

The design proposed in this thesis work is a two-dimensional (2D) photonic crystal structure consisting of hexagonal arrangement of air holes in silicon. This proposed structure can also be designed on SOI structure. The SOI platform provides additional benefits for the integration of photonic devices, such as low optical loss, low power consumption, high stability, and high speed. Since structure based on SOI offers the ease of fabricating the structure, thus future work can be done on SOI based structure.

The origin of the difference between the circular hole and elliptical hole PhC waveguide can be studied using the electromagnetic scattering pattern of circular and elliptical cylinders. This study would provide physical insight into the geometry (hole shape) dependence of loss characteristics of PhC waveguide based devices.

By default, the common trend is to use a circular hole pattern for PhC structures. The design investigations can be done in future resulting in different hole geometries which might results in better performances for certain applications. Having noted that, it could be possible to find the optimum hole geometry for wide band low loss applications. The work along this line of extension is worth exploring.

Also, the same structure can be designed for a layout having a complete band gap for both TE and TM polarization. In this case the device will work for both the polarizations i.e. TE and TM polarization.

In this thesis work we have used all-optical NAND gate to design the other basic optical logic gates but the same structure can also be designed by using the other universal optical logic gate i.e. the all-optical NOR gate.

Also, the proposed structure exhibits a response period of 6.48ps and bit rate of 0.154 Tb/sec. This bit rate can be improved by designing the structure on a smaller layout.

REFERENCES

[1] J. G. Fleming, Shawn-Yu Lin, "Three-dimensional photonic crystal with a stop band from 1.35 to 1.95 ,um" Optics Letters, Vol. 24, No. 1, January (1999).

[2] J. D. Joannopoulos, S. G. Johnson, J. N. Winn, R. D. Meade, "Photonic Crystals - Molding the low of light", 2nd Edition, Princeton University Press, 2008.

[3] L. Weng, "An Introduction to Photonic Crystals", LC Optics and Photonics Course, Kent State University, 2012.

[4] E. Yablonovitch, "Inhibited spontaneous emission in solid-state physics and electronics", Physical Review Letters, Vol. 58, pp. 2059−2062, 1987.

[5] J.D. Joannopoulos, P. R. Villeneuve & S. Fan, "Photonic Crystals: putting a new twist on light", Nature, Vol. 386, No. 6621, pp. 143-149, 1997.

[6] E. Yablonovitch, "Photonic Crystals", Phys. Rev. Lett. 58, p1059 (1987).

[7]Y. Akahane, T. Asano, B. S. Song, & S. Noda, "High-Q photonic nanocavity in a two-dimensional photonic crystal", Nature, Vol. 425, No. 6961, pp. 944-947, 2003.

[8] S. Prorok, "Nanophotonics and integrated optics: Photonic Crystal Cavities", CST AG, 2013.

[9] Pallavi Singh, Devendrs Kr. Tripathi, Shikha Jaiswal and H.K. Dixit, "All-optical logic gates:designs, classification, and comparison", Hindawi Publishing Corporation,Vol.2014.

[10] Yablonovitch E 1987 "Inhibited spontaneous emission in solid-state physics and electronics" *Phys. Rev. Lett.* 58, 2059–2062

[11] John S 1987 "Strong localization of photons in certain disordered dielectric superlattices" *Phys. Rev. Lett.* 58, 2486–2489

[12] Qiu M, Mulot M, Swillo M, Anand S, Jaskorzynak B, Karlsson A, Kamp M and Forchel A 2003 "Photonic crystal optical filter based on contra-directional waveguide coupling" *Appl. Phys. Lett.* 83, 5121– 5123

[13] Beggs D, White T, Cairns L, O'Faolain L, and Krauss T 2009 "Demonstration of an integrated optical switch in a silicon photonic crystal directional coupler" *Physica E* 41, 1111–1114

[14] Fekete L, Kadlec F, Kuzel P, and Nemec H 2007 "Ultrafast optoterahertz photonic crystal modulator" *Opt. Lett.* 32, 680–682

[15] Gu L, Jiang W, Chen X, Wang L, and Chen R T 2007, "High speed silicon photonic crystal waveguide modulator for low voltage operation" *Appl. Phys. Lett*. 90, 071105

[16] Jiang Y, Jiang W, Gu L, Chen T, and Chen R T 2005 "80-micron interaction length silicon photonic crystal waveguide modulator" *Appl. Phys. Lett.* 87, 221105

[17] Kosaka H, Kawashima T, Tomita A, Notomi M, Tamamura T, Sato T, and Kawakami S 1998 "Superprism phenomena in photonic crystals" *Phys. Rev. B* 58, R10096

[18] Amet J, Baida F, Burr G, and Bernal M.-P 2008 "The superprism effect in lithium niobate photonic crystals for ultra-fast, ultra-compact electro-optical switching" *Photonic. Nanostruct*. 6, 47–59

[19] Diziain S, Amet J, Baida F I, and Bernal M.-P 2008 "Optical far-field and near-field observations of the strong angular dispersion in a lithium niobate photonic crystal superprism designed for double (passive and active) demultiplexer applications" *Appl. Phys. Lett.* 93, 261103

[20] Lin S Y, Chow E, Bur J, Johnson S G, and Joannopoulos S J 2002 "Low-loss, wide-angle Y splitter at 1.6-_m wavelengths built with a two-dimensional photonic crystal," *Opt. Lett.*, vol. 27, no. 16, pp. 1400–1402

[21] Takeda H and Yoshino K 2003 "Tunable light propagation in Y-shaped waveguides in two-dimensional photonic crystals utilizing liquid crystals as linear defects," *Phys. Rev. B*, vol. 67, p. 073106

[22] Inoue K, Sugimoto Y, Ikeda N, Tanaka Y, Asakawa K, Sasaki H, and Ishida K 2004 "Ultra-small photonic-crystal-waveguide-based Y-splitters useful in the near-infrared wavelength region," *Jpn. J. Appl. Phys.*, vol. 43, no. 4A, pp. L 446–L 448

[23] A. Piccardi, A. Alberucci, U. Borotolozzo, S. Residori, G. Assanto, Appl. Phys. Lett. 96 (2010) 071104.

[24] L.X. Mu, W.S. Shi, T.P. Zhang, H.Y. Zhang, Y. Wang, G.W. She, Y.H. Gao, P.F. Wang, J.C. Chang, S.T. Lee, Appl. Phys. Lett. 98 (2011) 163101.

[25] H. Wei, Z.P. Li, X.R. Tian, Z.X. Wang, F.Z. Cong, N. Liu, S.P. Zhang, P. Nordlander, N.J. Halas, H.X. Xu, Nano Lett. 11 (2011) 471.

[26] Y.L. Fu, X.Y. Hu, C.C. Lu, S. Yue, H. Yang, Q.H. Gong, Nano Lett. 12 (2012) 5784.

[27] J.F. Tao, J. Wu, H. Cai, Q.X. Zhang, J.M. Tsai, J.T. Lin, A.Q. Liu, Appl. Phys. Lett. 100 (2012) 113104.

[28] P. Sahu, All-optical switch using optically controlled two mode interferencecoupler, Appl. Opt. 51 (2012) 2601–2605.

[29] Y.A. Zaghloul, A.R.M. Zaghloul, Complete all-optical processing polarization-based binary logic gates and optical processors, Opt. Express 14 (2006)9879–9895.

[30] J.Y. Kim, J.M. Kang, T.Y. Kim, S.K. Han, 10 Gbit/s all-optical composite logic gateswith XOR, NOR, OR and NAND functions using SOA-MZI structures, Electron.Lett. 42 (2006) 303–304.

[31] L. Zhang, Electro-optic directed logic circuit based on micro ring resonators forXOR/XNOR operations, Opt. Express 20 (2012) 11605–11614.

[32] Y. Tian, Proof of concept of directed OR/NOR and AND/NAND logic cir-cuits consisting of two parallel micro ring resonators, Opt. Lett. 36 (2011)1650–1652.

[33] Q. Xu, R. Soref, Reconfigurable optical directed-logic circuits using microresonators-based optical switches, Opt. Express 19 (2011) 5244–5259.

[34] T.K. Liang, High speed logic gate using two-photon absorption in silicon wave-guides, Opt. Commun. 256 (2006) 171–174.

LIST OF PUBLICATION:

Shiba Fatima, Preeti Rani, Yogita Kalra and R. K. Sinha, "**Design of all-optical logic gates using NAND gate in photonic crystal waveguides**", in **SPIE** conference OPTICS+PHOTONICS 2016: Photonic Fiber and Crystal Devices: Advances in Materials and Innovations in Device Applications X conference, **paper no. 9958-30** to be held in **SAN DIEGO**, CALIFORNIA, U.S. from 27th AUG to 1st SEPT 2016.